Jurnal
Teknologi

Full paper

Effect of Transition Metal Oxide Doping (Cr, Co, V) in the Photocatalytic Activity of TiO_2 for Congo Red Degradation under Visible Light

P. W. Koh[a], L. Yuliati[b], S. L. Lee[b]*

[a]*Department of Chemistry, Faculty of Science, Universiti Teknologi Malaysia, 81300 UTM Johor Bahru, Johor, Malaysia*
[b]*Ibnu Sina Institute for Fundamental Science Studies, Universiti Teknologi Malaysia, 81300 UTM Johor Bahru, Johor, Malaysia*

*Corresponding author: slllee@ibnusina.utm.my

Article history

Received :5 March 2014
Received in revised form :
19 April 2014
Accepted :3 May 2014

Graphical abstract

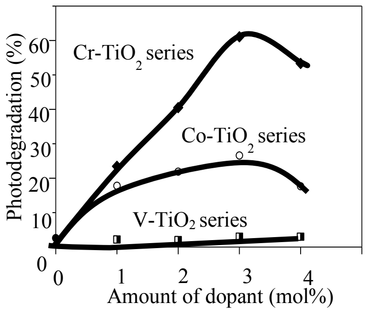

Abstract

Comparative study of Cr, Co or V-doped TiO_2 was carried out. The photocatalysts were synthesized via sol-gel method. The results indicated that the dopants of Cr, Co, and V induced anatase to rutile phase transition of TiO_2 at different dopant amounts of 1, 4, 2 mol%, respectively. Besides that, the existence of dopant extended the absorption wavelength of TiO_2 to visible light region, thus making it a visible-driven photocatalyst. The doped transition metal exhibited different oxidation states on the TiO_2 surface. The prepared photocatalysts were tested over photodegradation of Congo Red. Amongst all, Cr-doped TiO_2 (3 mol%) was the best photocatalyst attributed to the presence of 45% rutile phase, reduced band gap energy of 2.30 eV and formation of Cr^{6+}, which acted as an electron scavenger to delay the hole-electron recombination.

Keywords: Titania; transition metal oxide; congo red; photodegradation

Abstrak

Kajian perbandingan TiO_2 yang didop dengan Cr, Co atau V telah dijalankan. Kesemua fotomangkin telah disintesis melalui kaedah sol-gel. Keputusan menunjukkan bahawa Cr, Co, dan V mendorong peralihan fasa anatas kepada fasa rutil pada jumlah pendopan yang berbeza, iaitu pada 1, 4, 2 mol%. Selain itu, kewujudan pendopan melanjutkan penyerapan gelombang TiO_2 ke rantau cahaya nampak, justeru menjadikannya fotomangkin yang dipacu oleh cahaya nampak. Logam peralihan yang didopkan mempamerkan keadaan pengoksidaan yang berbeza pada permukaan TiO_2. Fotomangkin yang disediakan teleh diuji dalam fotodegradasi Congo Merah. Antaranya, TiO_2 yang didopkan dengan Cr (3 mol%) adalah fotomangkin yang terbaik disebabkan oleh kehadiran 45% fasa rutil, pengurangan jurang tenaga sehingga 2.30 eV dan kewujudan Cr^{6+}, yang bertindak sebagai pengaut elektron untuk melambatkan penggabungan semula lubang-elektron.

Kata kunci: Titania; logam peralihan; congo merah; fotodegradasi

■1.0 INTRODUCTION

Dyes are widely used in many industries such as textile, leather tanning, food industry, *etc*. It was reported that the amount of current world's dyestuffs production is about 10 million kg per year and between 1 to 2 million kg of active dyes have entered the biosphere, either dissolved or suspended in water [1]. Pollution caused by dye-containing wastewater towards the environment is of great concern associated with their toxicity to aquatic lives and mutagenic to human [2].

Advanced oxidation process (AOP) is emerging as a promising technology which has been successfully used to decompose many hazardous chemical compounds to acceptable levels, without producing sludge which requires further handling [3]. One of the novel examples of AOP is heterogeneous photocatalytic oxidation in which the process is characterized by the formation of hydroxyl radicals ($^{\cdot}OH$) and superoxide anion ($O_2{\cdot}^{-}$) when the photocatalyst is illuminated with light while in contact with oxygen and water. The active radicals able to degrade the toxic dye and fully mineralize them into non-toxic anionic compound were reported in many cases.

Among many semiconductors, such as TiO_2, ZnO, CdS, ZnS and Fe_2O_3, there is a general agreement that TiO_2 is more superior because it is resistance to chemical and photochemical corrosion, remains stable after repeated catalytic cycles and it is less expensive [4]. But, TiO_2 itself is yet a perfect photocatalyst. The anatase phase of TiO_2 has large band gap energy (3.2 eV) which renders it inactive under visible light irradiation. Besides, it experiences fast electron and hole recombination which results in poor photocatalytic activity. Many approaches have been done to modify TiO_2 such as metal coupling [5], dye sensitizer [6], transition metal doping [7]. Transition metal doping appears to be an effective method in enhancing the photocatalytic activity of titania. Chromium and vanadium are able to enhance the photocatalytic activity by delaying the combination of photogenerated electrons and holes [8,9] or enhancing the adsorption activity [10]. Conversely, poisonous effect of these doped metals have also been reported [11,12]. The contradicting results in many reported works could be due to different specific preparation methods and experimental conditions applied in the photocatalytic testing. Hence, it is difficult to compare the actual effects of transition metal on the TiO_2.

There are limited reports on the effect of metal dopants on the photocatalytic activity of TiO_2 under combinatorial approach using sol-gel as the synthesis method. In this study, three selected transition metal oxides, namely chromium oxide, cobalt oxide and vanadium oxides, doped TiO_2 were investigated in more detailed to get a deeper understanding of the effect of the dopants particularly on the structural, optical properties and speciation of doped transition metal on the effectiveness of TiO_2 to photodegrade dye. Chromium, cobalt or vanadium oxide was doped in/on titania via sol-gel method and the activities were tested by means of photodegradation of Congo Red (CR). CR was chosen because it consists of benzedine structure, which is possible to split into carcinogenic amines, yet is widely used in textile industry due to its effectiveness and low cost [13]. Therefore, removing CR via photodegradation method is of great interest.

■2.0 EXPERIMENTAL

Transition metal oxides doped titania photocatalysts were synthesized via sol-gel method. In a typical synthesis, titanium tetraisopropoxide (TTIP) (97%, Aldrich) was mixed with absolute ethanol (99.98%, HmBG) as solvent and acetylacetone (≥ 99%, Aldrich) as chelating agent according to the molar ratio 1: 100: 2 respectively to form a light yellowish clear solution and stirred for 60 minutes at room temperature. Chromium oxides were prepared separately by dissolving required amount of chromium(III) acetylacetonate (97%, Aldrich) in 1 – 5 mL of acetylacetone depending on the amount of chromium precursor. Then, it was added drop wise into the light yellowish solution. The mixture was stirred for another 30 minutes at room temperature and was then stirred under temperature at 353 K to evaporate the solvent. The gel was dried in the oven at 383 K overnight, ground into powder and lastly calcined at 773 K for 5 h. Cobalt and vanadium oxides doped TiO_2 were prepared via the same procedures except using cobalt(II) acetylacetonate (99%, Acros) and vanadylacetylacetonate (98%, Aldrich) as cobalt and vanadium oxides precursor, respectively. The molar ratio of the transition metal oxides in the photocatalyst was varied from 0.5 to 4 mol% for all doped titania series. Bare TiO_2 was prepared with same procedure without the addition of transition metal precursor. Samples were denoted as yM-TiO_2, where y refers to mol% of dopant M which is Cr, Co or V oxides.

The phases and crystallinity of the synthesized photocatalyst were examined via X-ray diffraction using Bruker Advance D8 X-ray diffractometer with Cu Kα radiation (λ = 0.15418 nm, 40 KV, 40 mA). The samples were scanned in the range from 2θ = 20 – 90 ° with a scan rate of 0.1°/s. Perkin Elmer Ultraviolet-visible Spectrometer Lambda 900 was used to record diffuse reflectance UV-visible (DR UV-Vis) spectra with barium sulfate ($BaSO_4$) as reference. Temperature Programme Analysis (TPR) was carried out on selected samples in a temperature range of 573 – 973 K on Micromeritics Auto Chem II 2920 chemisorption analyser. Prior to measurement, the samples were pretreated under N_2 gas flowing at 473 K for 15 minutes. Argon gas which contained 5.1% H_2 was passed through the sample tube during measurement with flowing rate of 25 cm^3/min.

The photocatalytic activity of the synthesized samples was evaluated through the photodegradation of CR. The prepared photocatalyst (0.1 g) was added to 50 mL of 100 ppm CR solution. The suspension was irradiated by a halogen fiber optic light illuminator (Dolan-Jenner MI 157, 150W) as visible light source and UV cut-off filter (Edmund Optics, 400 nm) was used to filter UV light. The solution was stirred in dark condition to ensure that the absorption has reached the equilibrium before light irradiation. The normal incidence of visible light with the solution was kept at a distance of 4 cm. After 24 h of light irradiation, the solution was filtered using a membrane syringe filter. The filtrate concentration was measured using UV-Vis spectrophotometer (ThermoFisher, Genesys 10S). The temperature of the reaction solution was maintained at 298 – 303 K by a flow of cooling water.

■3.0 RESULTS AND DISCUSSION

3.1 Structural Analysis

The structures of all synthesized materials were characterized via XRD and are depicted in Figure 1. The bare TiO_2 showed purely anatase phase (JCPDS 21-1272) which is the most active polymorph of titania. The diffraction peaks at 25.3, 37.2, 37.8, 38.7, 48.1, 53.9, 54.9 and 62.7 ° are assigned to lattice planes (1 0 1), (0 0 4), (2 0 0), (1 0 5), (2 1 1) and (2 1 3), respectively [13].

Generally, addition of these three metal oxide dopants suppressed the crystallinity of TiO_2 and induced anatase to rutile phase transition at different amount of dopant. It has been suggested that the sol-gel method facilitated incorporation of the doped transition metal into framework of TiO_2, thus changing the physical and chemical properties of TiO_2 photocatalyst. As observed, rutile phase (JCPDS 21-1276) can be seen starting at 1, 4, 2 mol%, respectively for Cr, Co, and V oxides doped TiO_2, respectively. This phenomenon could be related to the difference between the ionic size of dopant and Ti^{4+}. According to Hume-Rothery rules, the dopant is able to substitute Ti^{4+} if the difference in ionic radius of dopant and Ti^{4+} does not exceed 15%. In addition, it has been well accepted that dopant of lower charge than +4 and similar ionic radii to Ti^{4+} (0.605 Å) [15] is able to substitute Ti at the substitutional position and results in anatase-rutile phase transition [7, 16]. The composition percentage of both anatase and rutile phases are shown in Table 1. The trend of the ionic size nearer to Ti^{4+} (0.605 Å) is as follow: Cr^{3+} (0.615 Å), V^{4+} (0.58 Å), Co^{2+} (0.65 Å), Co^{3+} (0.545 Å) and lastly V^{5+} (0.54 Å) [14]. It able to explain why Cr^{3+} able to induce more rutile phase, up to 45% when TiO_2 was doped with 3 mol% Cr oxides. Further increment of Cr dopant gave no effect on the amount of rutile phase. On the other hand, the added cobalt could have most likely incorporated in the interstitial position of TiO_2 and consequently produced single anatase phase in the material for low concentration of cobalt precursor (less than 3 mol%). Higher concentration of cobalt precursor could serve as a driving force for Co^{2+} or Co^{3+} to incorporate, by means of not only at the interstitial position but also at the substitutional position of TiO_2 during the preparative calcination of sample [17], leading to anatase-rutile phase transition.

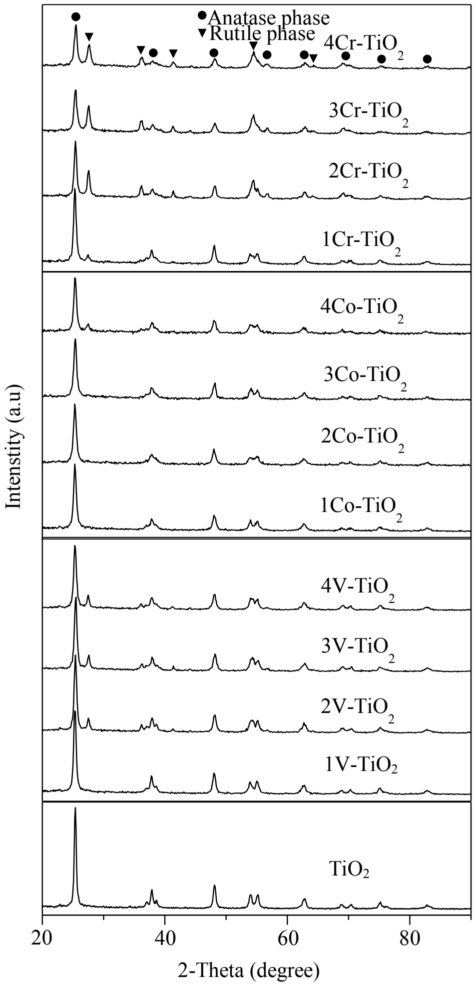

Figure 1 XRD patterns of Cr, Co and V doped TiO_2 and bare TiO_2

Table 1 Composition and band gap energy of Cr-TiO_2, Co-TiO_2 and V-TiO_2

Sample	Rutile (%)[a]	Anatase (%)[b]	Band gap (eV)[c]
TiO_2	n.a	100	3.25
1Cr-TiO_2	15	85	2.85
2Cr-TiO_2	39	61	2.35
3Cr-TiO_2	45	54	2.30
4Cr-TiO_2	41	58	2.20
1Co-TiO_2	n.a	100	3.15
2Co-TiO_2	n.a	100	2.85
3Co-TiO_2	n.a	100	2.50
4Co-TiO_2	22	78	2.25
1V-TiO_2	n.a	100	2.75
2V-TiO_2	20	80	2.00
3V-TiO_2	23	77	1.95
4V-TiO_2	24	76	1.80

[a] Calculated from Spurr equation
[b] Calculated from 100-rutile phase
[c] Calculated from Tauc plot

In V-doped TiO_2 series, anatase to rutile transformation started at 2 mol% V doped material. The result was in agreement with the previous statement which claimed vanadium doping led to transformation from anatase to rutile phase under heat treatment at 773 K [18]. It was also observed that amount of dopant did not have significant effect on the intensity of the rutile peak as the intensity of the rutile peaks ranging 20 to 24%, even though the amount of dopant was increased from 1 to 4 mol%. This can be explained in term of the valance state of the ion. The ionic radius of vanadium ions (V^{4+} = 0.580 Å, V^{5+} =0.540 Å) is smaller than Ti^{4+} (0.605 Å) which enabled some of the added vanadium to substitute titania. Every 4 doping of V^{5+} in the Ti^{4+} octahedral cationic site led to one Ti^{4+} cation vacancy. However, as the dopant amount increases, accommodation of excess cation vacancy does not seem to be favorable in anatase structure [19]. As a result, the vanadium oxide might be separated out from the crystal structure of TiO_2. It explained why the rutile phase percentage was independent on the amount of dopant added. Nevertheless, the amount of all the dopants might be still too little to be detected by XRD as no peaks attributed to these dopants were detected.

3.2 Absorption Properties

Bare TiO_2 exhibited as a white color powder while Cr-TiO_2, Co-TiO_2 and V-TiO_2were light brownish orange, light green and grey color powder, respectively. Besides, the color becomes more intense with the increasing of amount of dopant. Figure 2 depicts the absorption spectra of the prepared photocatalysts.

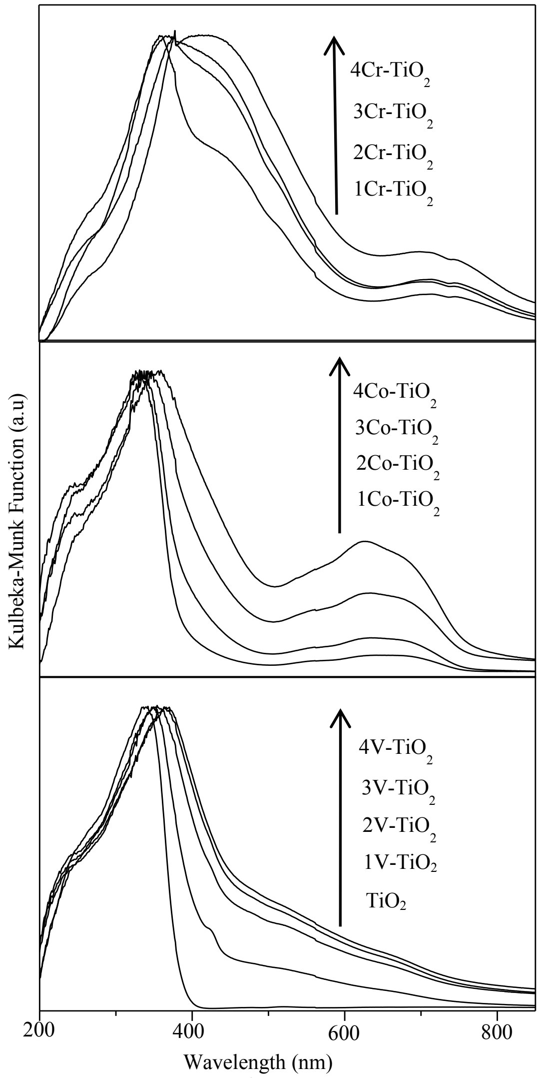

Figure 2 DR UV-Vis spectra of samples in Cr, Co and V doped TiO_2series and bare TiO_2

Bare TiO_2 predominantly shows two absorption peaks at around 280 – 330 nm and a shoulder at 230 – 280 nm, which are assigned to the charge transfer between O^{2-} and the octahedral Ti sites, and tetrahedral Ti sites, respectively [20]. Doping with Cr, Co, and V oxides has caused peak shifting at around 380 nm. The most significant shifting was observed in Cr-TiO_2 series, indicating that Cr can be easily substituted into Ti matrix. This result is consistence with XRD data above. From the UV-Vis spectra of Cr-TiO_2, other than absorption peak of TiO_2, addition broad peak at 600 – 800 nm was observed which is attributed to $^4A_{2g}\rightarrow{}^4T_{2g}$ d-d transitions of Cr^{3+} [21]. Jaimy *et al.* [22] reported that peaks in this range was associated with $Cr^{3+}\rightarrow Ti^{4+}$ charge transfer, *i.e.*, excitation of electron of Cr^{3+} to conduction band of TiO_2. A shoulder around 450 nm is assigned to $^4A_{2g}\rightarrow{}^4T_{1g}$ of Cr^{3+} in an octahedral environment.

Doping of cobalt oxide resulted in formation of shoulder near 400 nm, strongly suggesting the presence of Co^{3+}. Meanwhile, a broad peak around 600 nm was ascribed to Co^{2+} and Co^{3+} [23, 24]. In the cobalt oxides doped titania samples, broad peak at 600 nm was found to increase proportional with the increasing amount of cobalt oxides doping. Similarly, doping with vanadium oxides resulted in peak shifting around 390 nm and formation of new absorption peak and tailing of absorption curves reveal that V-TiO_2 absorb the photon energy in the range of 400 – 800 nm. It was reported that V^{5+} has absorption at < 579 nm, and V^{4+} has an absorption band at around 770 nm [25,26]. In addition, tailing of absorption band was correlated to the charge-transfer transition from the d-orbital of V^{4+} to the conduction band of TiO_2 [19].

It was documented that the absorption at the visible light region of modified TiO_2 around 440 nm and 486 nm may be ascribed to the oxygen vacancies which give rise to colored center [27, 28]. In present study, formation of oxygen vacancies as a result of substitution of Ti^{4+} with different valence states of dopants was confirmed by the formation of rutile phase. Hence, the observed new absorption peaks at the visible region after addition of dopants (Cr, Co and V) could be attributed to both oxygen vacancies and new impurity level formed by the dopant within the TiO_2.

Band gap energy is always one of the main criteria for a photocatalyst as smaller band gap energy of enable photocatalyst to utilize visible light from the solar system. The band gap energy of the Cr-TiO_2, Co-TiO_2 and V-TiO_2 were calculated from the Tauc Plots and the results are shown in Table 1. As can be seen, a significant lowering of band gap energy of $TiO_2$was observed with increasing amount of dopants. The absorption in the visible light region indicated the prepared samples could be visible-light-driven photocatalysts.

3.3 TPR Analysis

The species of transition metal on the TiO_2 surface was determined via TPR study. This study is important to understand the species presence that will affect the photocatalytic activity by trapping the electron as well as the interaction between the dye and the photocatalyst. TPR profiles of the prepared samples are shown in Figure 3. Both 1Cr-TiO_2 and 3Cr-TiO_2 showed a shoulder at around 673 K and an intense absorption peak at 825 K which are corresponding to reduction of Cr^{6+} to Cr^{3+} and Cr^{3+} to Cr^{2+}, respectively [29]. Therefore, the reduction peaks at 673 and 825 K validated the presence of Cr^{6+} and Cr^{3+}, respectively in the samples even though Cr(III) precursor was used in the present study. Similar finding was reported by Reddy *et al.* [29]. As for TPR profiles of 1Co-TiO_2 and 3Co-TiO_2, only one reduction peak was detected at 795 K and 764 K, respectively. This reduction peak was attributed to stepwise reduction of cobalt oxide via $Co^{3+}\rightarrow Co^{2+}\rightarrow Co^0$ and the steps were overlapped. The similar phenomenon was detected when the Co doped TiO_2 was derived from an organic precursor [30]. It was observed that the reduction temperature decreased with the increasing of the amount of Co dopant. This could be due to more interaction between Co and Ti which subsequently increased the reducibility of the Co species.

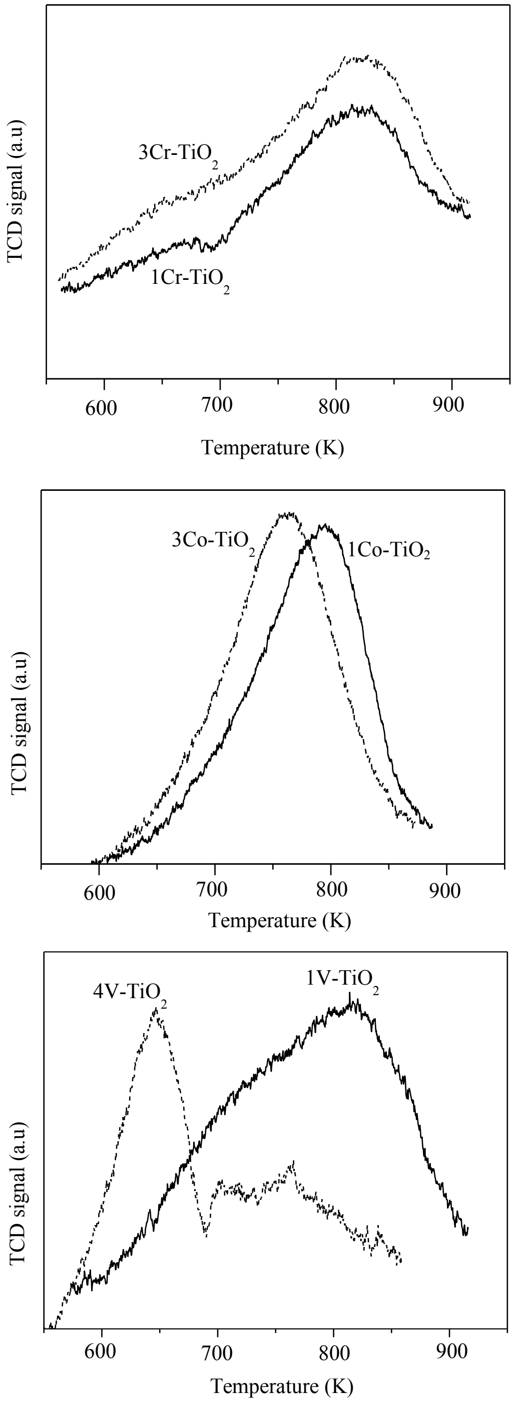

Figure 3 TPR profiles of selected samples in Cr, Co or V-doped TiO_2 series

On the other hand, it was clearly seen that 1V-TiO_2 gave only one reduction peak at 814.3 K which was corresponding to reduction of V_6O_{13} to V_2O_4, indicating V^{4+} existed dominantly in the sample 1V-TiO_2. As the amount of V dopant increased to 4 mol%, a peak of lower reduction temperature at 647.4 K in 4V-TiO_2 was obtained. This peak was associated with reduction of V_2O_5 to V_6O_{13}, hence it was a good indication of existence of V^{5+} species. The detection of this peak is always linked to formation of strong interaction between V species and the H_2 gas due to V-O-Ti bonds of higher reducibility. Besides, a hump at 765.1 K was also observed in 4V-TiO_2, implying presence of trace V^{4+} species [31].

3.4 Photocatalytic Testing

The prepared Cr-, Co-, and V-doped TiO_2samples were subjected for photocatalytic testing with CR used as the model reaction. The net photodegradation (after exclude the absorption in the dark) is shown in Figure 4. Bare TiO_2 gave a negligible activity of 2.61% of phototodegradation. Addition of Cr and Co enabled TiO_2 active under visible light and is in agreement with the DR-UV-Vis spectra shown in Figure 2. In addition, Cr and Co greatly enhanced the photocatalytic degradation of CR, with highest activity of 61% and 26%, respectively by 3Cr-TiO_2 and 3Co-TiO_2. The enhancement of photocatalytic activity could be due to Cr and Co act as an electron trapper [32]. The reduction potential of Cr^{6+} to Cr^{3+} and Co^{3+} to Co^{2+} is 1.38 eV and 1.92 eV, respectively, which is more positive than the conduction band (CB) of TiO_2. Therefore, Cr and Co dopant could accept electron from CB and reduced the electron and hole recombination rate. Besides, the presence of rutile phase in 3Cr-TiO_2 might be able to further reduce the electron hole recombination rate [33, 34]. The optimum percentage of rutile phase of 40 wt% was reported [33] and the value is similar to the percentage of rutile in the 3Cr-TiO_2 photocatalyst. However, further addition of Cr and Co dopant hampered the activity which might be due to blockage of the active site by the excess dopants. Alternatively, the excess dopant might have acted as a hole-electron recombination centre.

On contrary, V dopant did not enhance the photocatalytic activity of TiO_2. It was reported that V formed mainly as a bulk outside TiO_2 surface when the hydrolysis of Ti precursor took 1 hour prior to addition of V dopant [11]. Due to the similar synthesis procedure applied in the current work, it was hence believed that the bulk V structure was formed in the V-doped TiO_2. The bulk V caused “poisonous effect” in photodegrading CR resulting in weak photocatalytic activity.

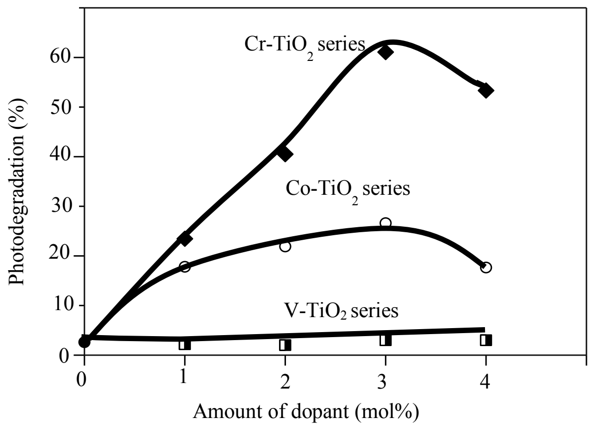

Figure 4 Photodegradation of Congo Red by different transition metal oxides doped TiO_2 at different amount of dopant. (irradiation time = 24 hours, initial concentration of dye = 100 ppm)

4.0 CONCLUSION

Cr, Co or V doped TiO_2 had been successfully synthesized via sol-gel method. The addition of 1 mol% of Cr, 4 mol% of Co and 2 mol% of V dopant into TiO_2 had induced anatase-rutile phase transformation. The metal oxides doping had also extended the absorption wavelength to visible light region and reduced the band gap energy of the material. The relatively high rutile phase composition in Cr-doped TiO_2 materials contributed greatly to their excellent photocatalytic performance in Congo Red photodegradation under visible light irradiation. Metal ions of higher oxidation states, *e.g.* Cr^{6+} and Co^{3+}, were detected in Cr- and Co-doped TiO_2 materials and these ions were believed to reduce the electron-hole recombination rate by trapping the electron generated. Even though the lowest band gap energy of 1.80 eV was achieved in 4V-TiO_2, the formation of bulk V in the material has given negative effect to its photocatalytic activity. It has been demonstrated that the Cr-doped TiO_2 materials have the highest photocatalytic activity, followed by Co-doped TiO2 and V-doped TiO_2 materials.

Acknowledgement

The authors gratefully acknowledge the Ministry of Higher Education Malaysia (MOHE) and Universiti Teknologi Malaysia (UTM) for the Research University Grant (vote no.: Q.J.130000.2526.03H90). The authors are also thankful to the Ministry of Science, Technology and Innovation Malaysia (MOSTI) for the MyPhD scholarship.

References

[1] S. J. Allen, Q. Gan, R. Matthews, P. A. Johnson. 2003. *Bioresour. Technol.* 88: 143.
[2] S. Meric, D. Kaptan, T. Olmez. 2004. *Chemosphere.* 54: 435.
[3] F. Han, V. S. R. Kambala, M. Srinivasan, D. Rajarathnam, R. Naidu. 2009. *Appl. Catal. A.* 359: 25.
[4] R. Thiruvenkatachari, S. Vigneswaran, S. Moon. 2008. *Korean J. Chem. Eng.* 25: 64.
[5] A. H. Zyoud, N. Zaatar, I. Saadeddin, C. Ali, D. Park, G. Campet, H. S. Hilal. 2010. *J. Hazard. Mater.* 173: 318.
[6] P. Chowdhury, J. Moreira, H. Gomaa, A.K. Ray. 2012. *Ind. Eng. Chem. Res.* 51: 4523.
[7] J. Choi, H. Park, M.R. Hoffmann. 2010. *J. Phys. Chem. C.* 114: 783.
[8] S. Zhang, Y. Chen, Y. Yu, H. Wu, S. Wang, B. Zhu, W. Huang, S. Wu. 2008. *J. Nanopart. Res.* 10: 871.
[9] H. Hamdan, M.N.M. Muhid, S.L. Lee, Y.Y. Tan. 2009. *Inter. J. Chem. React. Eng.* 7, Article 4.
[10] X. Liang, S. Zhu, Y. Zhong, J. Zhu, P. Yuan, H. He, J. Zhang. 2010. *Appl. Catal. B: Environ.* 97: 151.
[11] M. Bettinelli, V. Dallacasa, D. Falcomer, P. Fornasiero, V. Gombacc, T. Montini, L. Romano, A. Speghini. 2007. *J. Hazard. Mater.* 146: 529.
[12] K. Wilke, H. D. Breuer. 1999. *J. Photochem. Photobiol. A-Chem.* 121: 49.
[13] A. Pielesz, A. Weselucha-Birczynska. 2000. *J. Mol. Struc.* 555: 325.
[14] C. T. Hsieh, W. S. Fan, W. Y. Chen, J. Y. Lin. 2009. *Sep. Purif. Technol.* 67: 312.
[15] R.D. Shannon. 1976. *Acta Cryst.* A32: 751.
[16] R. Arroyo, G. Cordoba, J. Padilla, V. H. Lara. 2002. *Mater. Lett.* 54: 397.
[17] J.M. Herrmann, J. Disdier, G. Deo, I. E. Wachs. 1997. *J. Chem. Soc.* 93: 1655.
[18] H. Li, G. Zhao, Z. Chen, G. Han, B. Song. 2010. *J. Colloid Interf. Sci.* 344: 247.
[19] K. Nagaveni, M. S. Hegde, G. Madras. 2004. *J. Phys. Chem. B.* 108: 20204.
[20] E. Astorino, J. B. Peri, R.J. Willey, G. Bisca. 1995. *J. Catal.* 157: 482.
[21] D. Dvoranová, V. Brezová, M. Mazúra, M. A. Malati. 2002. *Appl. Catal. B* 37: 91.

[22] K. B. Jaimy, S. Ghosh, S. Sankar, K. G. K. Warrier. 2011. *Mater. Res. Bull*. 46: 914.
[23] J. Wang, S. Uma, K. J. Klabunde. 2004. *Appl. Catal. B*. 48: 151.
[24] J. J. Li, S.Q. Liu, Y. Y. He, J. Q. Wang. 2008. *Micropor. Mesopor. Mater*. 115: 416.
[25] R. Asahi, T. Morikawa, T. Ohwaki, K. Aoki, Y. Taga. 2001. *Science*. 293: 269.
[26] K. Bhattacharyya, S. Varma, A. K. Tripathi, S. R. Bharadwaj, A. K. Tyagi. 2008. *J. Phys. Chem. C*. 112: 19102.
[27] N. Serpone. 2006. *J. Phys. Chem B*. 110: 24287.
[28] V. N. Kuznetsov, N. Serpone. 2006. *J Phys Chem B* 110: 25203.
[29] E.P. Reddy, L. Davydov, P.G. Smirniotis. 2002. *J. Phys. Chem. B*. 106: 3394.
[30] K. Suriye, P. Praserthdam, B. Jongsomjit. 2005. *Ind. Eng. Chem. Res*. 44: 6599.
[31] S. C. Shekar, K. Soni, R. Bunkar, M. Sharma, B. Singh, M. V. S. Suryanarayana, R. Vijayaraghavan. 2011. *Appl. Catal., B*. 103: 11.
[32] M. A. Rauf, M. A. Meetani, S. Hisaindee. 2011. *Desalin.* 276: 13.
[33] K.V. Baiju, A. Zachariah, S. Shukla, S. Biju, M.L.P. Reddy, K.G.K. Warrier. 2009. *Catal. Lett.* 130: 130.
[34] R. G. Nair, S. Paul, S. K. Samdarshi. 2011. *Sol. Energy Mater. Sol. Cells*. 95: 1901.